Acta Crystallographica Section D
Biological Crystallography
ISSN 0907-4449

Crystallization and preliminary neutron analysis of the dissimilatory sulfite reductase D (DsrD) protein from the sulfate-reducing bacterium *Desulfovibrio vulgaris*

Toshiyuki Chatake,[a] Nobuhiro Mizuno,[b] Gerrit Voordouw,[c] Yoshiki Higuchi,[d] Shigeki Arai,[a] Ichiro Tanaka[a] and Nobuo Niimura[a]*

[a]Neutron Structural Biology, Neutron Science Research Center, Japan Atomic Energy Research Institute, Tokai, Ibaraki 319-1195, Japan, [b]Department of Chemistry, Graduate School of Science, Kyoto University, Sakyo, Kyoto 606-8502, Japan, [c]Department of Biological Sciences, The University of Calgary, Alberta T2N 1N4, Canada, and [d]Department of Life Science, Graduate School and Faculty of Science, Himeji Institute of Technology, Koto, Kamigori, Ako-gun, Hyogo 678-1297, Japan

Correspondence e-mail: niimura@kotai3.tokai.jaeri.go.jp

Received 8 August 2003
Accepted 17 September 2003

Dissimilatory sulfite reductase D (DsrD) from *Desulfovibrio vulgaris* has been crystallized for a neutron diffraction study. The initial crystals obtained were too small for the neutron experiment. In order to obtain a larger crystal (>1 mm^3), a combination of two techniques was developed to determine the optimum crystallization conditions: a crystallization phase diagram was obtained, followed by crystal-quality assessment *via* X-ray diffraction. Using conditions determined in this manner, a large single crystal (1.7 mm^3) of DsrD protein was subsequently grown in D_2O solution by the macroseeding technique. A neutron diffraction experiment was carried out using the BIX-3 diffractometer at the Japan Atomic Energy Research Institute (JAERI), collecting data to 2.4 Å resolution from an optimized crystal.

1. Introduction

It is well known that the hydrogen-bonding networks around DNA-binding proteins play important roles in DNA–protein recognition. The protein interacts with the nucleic acid by direct hydrogen bonds as well as by water-mediated hydrogen bonds and achieves specific and precise DNA recognition in this manner. However, details of these hydrogen-bonding networks are not known because the conventional methods for structural study, X-ray crystallography and NMR spectroscopy, have difficulty in determining the positions of H atoms. In particular, X-ray analysis of H-atom positions requires a crystal of sufficient quality to diffract to ∼1.0 Å resolution. It is, however, very difficult to obtain such a good crystal in biological crystallography. Neutron scattering factors for H and D atoms ($b_H = -0.38$ and $b_D = 0.67$) are comparable to those of the non-H atoms in proteins ($b_C = 0.66$, $b_N = 0.94$, $b_O = 0.58$ and $b_S = 0.28$). Consequently, H and D atoms can be observed at medium resolution by neutron analysis (Schoenborn, 1985; Helliwell, 1997; Niimura, 1999; Tsyba & Bau, 2002). Recently, Habash and coworkers succeeded in identifying H and D atoms in a concanavalin A crystal at 2.4 Å resolution (Habash *et al.*, 2000). Dissimilatory sulfite reductase D (DsrD) from the sulfate-reducing bacterium *Desulfovibrio vulgaris* is a small protein composed of 78 amino acids. Dissimilatory sulfite reductases A and B, the genes for which are located immediately upstream from the *dsrD* gene, participate in sulfate respiration. However, DsrD does not possess high-affinity binding for sulfite or sulfide (Hittel & Voordouw, 2000), but has a B- and Z-DNA binding motif (Mizuno *et al.*, 2002, 2003). We are trying to determine the hydrogen-bonding networks of this protein (including the positions of the H atoms) using neutron crystallographic analysis in order to better understand the details of its DNA recognition.

To date, only about 20 neutron crystal structures of proteins have been determined, as a crystal larger than 1 mm^3 is necessary for neutron protein crystallography (Niimura *et al.*, 2003). The DsrD protein has already been crystallized for X-ray analysis (Mizuno *et al.*, 2000); however, the size of the crystal used in that study (0.4 mm^3) was insufficient for neutron diffraction. It is said that large crystals can be grown under conditions similar to those that produce high-quality crystals. We found that suitable conditions could be found by systematically adopting a combination of two techniques: (i) the use of a crystallization phase diagram and (ii) the evaluation of crystal quality through quantitative analysis of X-ray diffraction patterns. The crystallization phase diagram gives some preliminary information about conditions under which crystals can grow. Crystal-quality analysis using X-rays then allows the investigation to determine which are the best crystals. Using this approach, a large single crystal of DsrD was subsequently obtained in D_2O solution using the macroseeding technique. A neutron diffraction experiment was then carried out using the BIX-3 diffractometer (Tanaka *et al.*, 2002) at the Japan Atomic Energy Research Institute (JAERI).

Table 1
Statistics of X-ray experiments.

Values in parentheses are for the highest resolution shell.

Crystallization condition	1	2	3	4	5	6
Volume (mm^3)	0.16	0.14	0.09	0.04	0.04	0.03
Dimensions (mm)	0.07 × 0.50 × 0.45	1.00 × 0.40 × 0.35	1.50 × 0.40 × 0.15	0.40 × 0.35 × 0.30	0.65 × 0.30 × 0.20	0.65 × 0.35 × 0.15
Experimental						
Exposure time (min per frame)	20	20	20	20	20	30
Total frames	120	102	146	200	120	180
Space group	$P2_12_12_1$	$P2_12_12_1$	$P2_12_12_1$	$P2_12_12_1$	$P2_12_12_1$	$P2_12_12_1$
Unit-cell parameters						
a (Å)	60.5	60.6	60.5	60.4	60.5	60.5
b (Å)	65.1	65.1	65.1	65.0	65.1	65.1
c (Å)	46.5	46.6	46.6	46.6	46.6	46.6
Results						
Resolution (Å)	1.85	1.80	1.85	2.00	1.95	2.05
Overall B factor ($Å^2$)	17.9	13.8	18.0	20.1	17.8	20.3
R_{merge} (%)	3.5 (23.4)	3.4 (24.1)	3.7 (24.0)	4.2 (20.2)	4.2 (21.7)	5.4 (23.9)
Completeness (%)	95.0 (94.6)	93.7 (92.8)	91.4 (88.2)	92.0 (72.3)	97.0 (96.7)	97.1 (97.2)
$I/\sigma(I)$	55.7 (8.9)	52.9 (8.1)	59.2 (9.9)	53.4 (8.8)	45.7 (10.1)	43.4 (10.8)

2. Materials and methods

2.1. Sample preparation

The DsrD protein was produced and purified as reported previously (Hittel & Voordouw, 2000). Because the incoherent neutron scattering length of hydrogen is high, the presence of hydrogen increases the background noise in a neutron scattering experiment. Therefore, the H atoms in our protein crystals were replaced with deuterium as far as possible in order to reduce the high background noise. Accordingly, the sample of DsrD protein used in our experiment, which was originally prepared in H_2O solution with 20 m*M* Tris–HCl pH 7.2 and 0.1 *M* NaCl, was dialyzed against D_2O solution with the same components for 2 d and then stored for more than four months at 279 K prior to crystallization. Most of the exchangeable H atoms in DsrD had been replaced with D atoms; the time for H/D exchange was longer than usual (approximately several weeks).

2.2. Crystallization phase diagram

In the present study, the crystallization of DsrD was carried out in D_2O solution at 293 K by the sitting-drop vapour-diffusion method. Droplets with a volume of 4 µl were prepared by mixing equal volumes of 11.5–46.0 mg ml^{-1} protein solution and fully saturated deuterated ammonium sulfate (d-AS) solution and were equilibrated against reservoir solutions containing 1 ml 60–80% saturated d-AS solution (the pH of which had previously been adjusted to 5.3). The initial conditions were set up according to the previously successful crystallization conditions for X-ray samples in H_2O solution (Mizuno *et al.*, 2000). A two-dimensional crystallization phase diagram, in which the protein (DsrD) concentration and precipitant (d-AS) concentration were varied, was then determined (Fig. 1). Evaluation of the successful crystallization conditions was accomplished by observing the droplets for two months with a microscope; most crystals of DsrD appeared within this period.

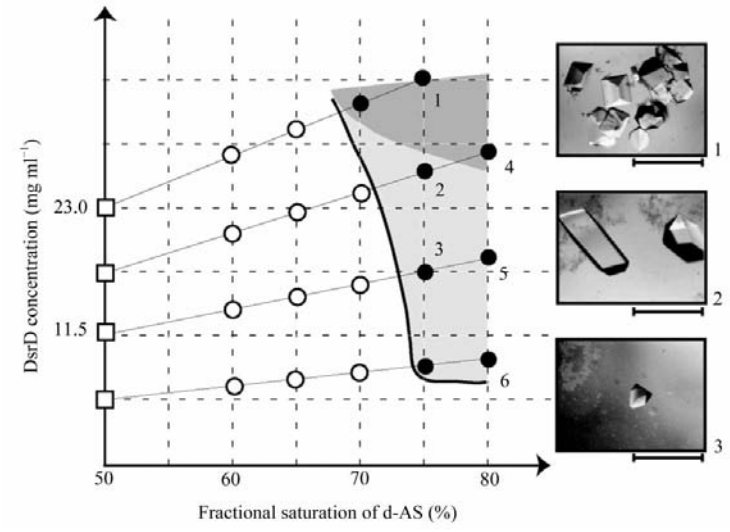

Figure 1
The crystallization phase diagram of DsrD obtained from vapour-diffusion experiments. The solid curve in this diagram is the nucleation curve. The vertical axis is the DsrD protein concentration, while the horizontal axis is the concentration of saturated ammonium sulfate in D_2O (d-AS). The squares show the initial conditions of the crystallization solution and the circles show the final (equilibrated) conditions. The open or closed circles correspond to the absence or presence of crystals, respectively, after two months. The region of fast crystal growth (first appearance within 2 d) is indicated by the dark grey area, while slow crystal growth (2–10 d) is shown as a light grey area. The numbers correspond to the actual crystals used for quality analysis in the subsequent X-ray experiment. Pictures of three sets of typical crystals are shown at the right of this figure (grown under conditions corresponding to points 1, 2 and 3). The scale bars are 1 mm.

2.3. X-ray experiment

Assessment of the crystal quality was subsequently carried out by an X-ray diffraction experiment. Six crystals grown under different crystallization conditions (shown as numbered points in Fig. 1) were used for the experiment. They were sealed in quartz capillaries (diameter = 1.0–1.5 mm) with mother liqour and mounted on the goniometer. The X-ray diffraction experiment was performed at 293 K on a DIP-2020 X-ray diffractometer (MacScience Inc.). The X-ray beam was Cu $K\alpha$ radiation (with diameter = 0.6 mm) generated by a rotating-anode generator operating at 50 kV and 100 mA and monochromated using a graphite monochromater. X-ray diffraction images were collected by the oscillation method with an oscillation angle of 1.0° per frame. The exposure time was 20 min per frame except for crystal 6, which was so small that an exposure time of 30 min per frame was used. More than 100 diffraction images were collected for each data set and the data collection was terminated when about 90% of the independent reflections had been covered. The data sets were individually processed with the programs *DENZO* and *SCALEPACK* from the *HKL* program package (Otwinowski & Minor, 1997). The statistics of the X-ray experiments are summarized in Table 1.

2.4. Macroseeding

After the crystal with the best diffraction quality had been selected (crystal 2 in Fig. 1), a macroseeding procedure based on these starting conditions was employed in order to obtain a large crystal for the neutron study. Firstly, a 20 µl droplet containing 17.3 mg ml^{-1} DsrD and 50% saturated d-AS

was pre-equilibrated against a reservoir containing 1 ml 75% saturated d-AS solution. After 48 h, the droplet was about 90% equilibrated (25.3 mg ml^{-1} DsrD, 72.5% d-AS). Next, a seed crystal previously grown in a 10 µl droplet (0.3 mm^3) was picked up and washed three times for 10–30 s in 77.5% d-AS solution. Finally, the seed was transferred to the pre-equilibrated droplet. The seed crystal gradually increased in size for about two weeks. This procedure was repeated four times until the crystal attained its final size (1.7 mm^3).

2.5. Neutron experiment

The large crystal obtained was sealed in an NMR sample capillary together with a small amount of the D_2O crystallization solution for the neutron experiment. Neutron diffraction data were collected at room temperature using a monochromatic neutron beam (λ = 2.88 Å) with the BIX-3 instrument in reactor JRR-3M at JAERI (Tanaka *et al.*, 2002). A total of 512 still diffraction patterns were recorded on a neutron-imaging plate at intervals of 0.3°. Exposure time was about 2 h per frame and the total time of measurement was 70 d. The diffraction patterns were processed with the programs *DENZO* and *SCALEPACK* (Otwinowski & Minor, 1997), which were modified for neutron diffraction.

3. Results and discussion

3.1. Crystallization

Fig. 1 illustrates the nucleation curve of DsrD in the crystallization phase diagram, showing the conditions under which crystals of DsrD appeared. Strictly speaking, this curve is not the same as a solubility curve, which is a very common term used in crystal-growth physics (Riès-Kautt & Ducruix, 1992). In principle, there are three zones in the crystallization phase diagram corresponding to undersaturation, metastable and nucleation. In the undersaturation zone, crystals never appear. In the metastable zone, crystals grow but nucleation does not occur (in other words, crystals only grow when seeds are present). In the nucleation zone, both crystal growth and new nucleation occur. The solubility curve is the boundary between the undersaturated and the metastable zones, while the nucleation curve (shown in Fig. 1) divides the metastable and the nucleation zones.

3.2. X-ray experiment

Fig. 2 shows the results of the X-ray experiments for quality analysis. Various parameters have been used to evaluate crystal quality in X-ray analysis. Resolution, $I/\sigma(I)$, $R_{\rm merge}$ and mosaicity are popular criteria; however, they are influenced by various experimental conditions such as crystal size, X-ray source, detector and exposure time. On the other hand, the overall B factor, which reflects disorder and mobility within the individual molecules that make up the crystal, is independent of experimental conditions. In the present analysis, two different criteria, the resolution and the overall B factor, were used for the assessment of crystals. The definition of the maximum resolution is where the $R_{\rm merge}$ value is about 25% for the outermost resolution shell. The overall B factors were estimated from a Wilson plot (Wilson, 1942) using data in the 3.5–2.0 Å resolution range and the *CCP*4 program suite (Collaborative Computational Project, Number 4, 1994). Fig. 2(*b*) shows that these two factors, the maximum resolution and the overall B factor, are positively correlated. Accordingly, we used the overall B factor as the more sensitive parameter for the assessment of the crystal quality. Our results indicate that condition 2 of Fig. 2(*a*) is the best of the six conditions that were evaluated. To our surprise, 2 was not at the lowest supersaturation ratio but in the middle of the crystallization phase, an unexpected result because it is generally thought that good crystals grow slowly in this region. The present analysis shows that good-quality crystals grew near 2 in the crystallization phase diagram (1, 3 and 5), while poor-quality crystals grew under conditions remote from 2 (4 and 6). Thus, we found that the assumption that good crystals grow at a low supersaturation ratio (*e.g.* crystals from point 6) is not always true.

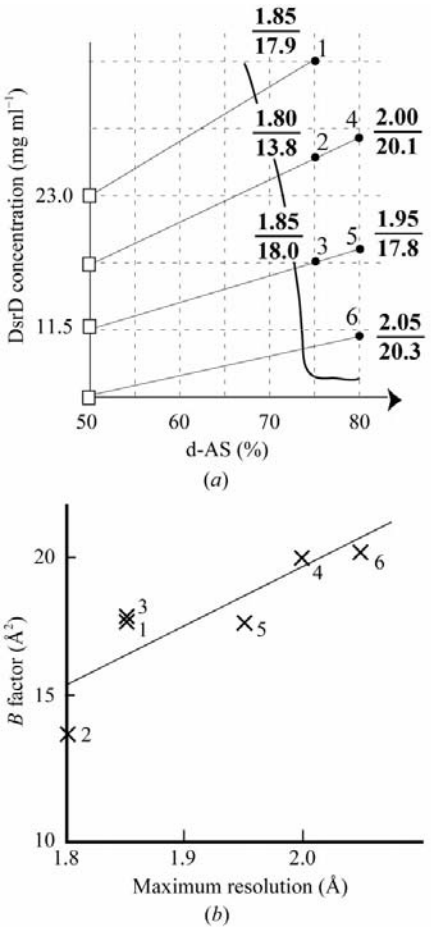

Figure 2
The results of the assessment of the crystal quality from analysis of X-ray diffraction patterns. (*a*) The maximum resolution and the overall B factor are shown superimposed on the crystallization phase diagram. In each case, the numerator indicates the maximum resolution of the diffraction patterns (Å), while the denominator indicates the overall B factor (Å^2). (*b*) The correlation between the maximum resolution and the overall B factor.

Table 2
Statistics of the neutron experiment.

Values in parentheses are for the highest resolution shell.

Data measurement	
Source	Nuclear reactor JRR-3M
Instrument	BIX-3
Wavelength (Å)	2.88
Space group	$P2_12_12_1$
Unit-cell parameters (Å)	a = 60.5, b = 65.1, c = 46.5
Resolution (Å)	100–2.4 (2.49–2.40)
Unique reflections	6740 (534)
$I/\sigma(I) > 1$	6481 (521)
Multiplicity	3.1 (2.7)
$R_{\rm merge}$ (%)	14.3 (39.5)
Completeness (%)	92.5 (82.1)
$I/\sigma(I)$	5.7 (2.3)
Preliminary analysis	
Resolution (Å)	20–2.4
Reflections used for refinement	6234
Reflections used for cross-validation	767 (10.1%)
R factor (%)	28.2
$R_{\rm free}$ (%)	30.1

3.3. Macroseeding

The subsequent macroseeding experiment using the vapour-diffusion method was carried out under crystallization condition 2. After a fourfold repetition of the macroseeding procedure, a crystal of 1.7 mm^3 was obtained. The total time required for macroseeding was two months. It is concluded that the nucleation curve (Fig. 1) and crystal-quality data (overall B factors of the diffraction patterns of crystals; Fig. 2) can provide useful starting parameters for

the growth of large crystals by the macro-seeding technique.

3.4. Neutron experiment and preliminary analysis

The DsrD protein crystallizes in space group $P2_12_12_1$, with unit-cell parameters a = 60.5, b = 65.1, c = 46.5 Å. The neutron diffraction patterns were processed to a resolution of 2.4 Å. A total of 6740 independent reflections were merged from 20 364 observed reflections, yielding an overall $R_{\rm merge}$ value of 14.3% (39.5% in the outermost shell). The completeness of the data was 92.5% for the entire data set and 82.1% for the 2.49–2.40 Å resolution range (the highest shell). The statistics for the neutron experiment are shown in Table 2. The initial phases were determined by the molecular-replacement method using the program *CNS* (Brünger *et al.*, 1998) with the coordinates of DsrD obtained by X-ray crystal analysis as an initial model (Mizuno *et al.*, 2003). Before least-squares refinement, the D atoms of the main polypeptide chain and selected H atoms whose positions could be estimated stereochemically were added to the model. An unbiased R factor ($R_{\rm free}$) was calculated for a subset of reflections (10%) which were omitted during the refinement and used to monitor its convergence. After the first refinement, the R factor was 28.2% ($R_{\rm free}$ = 30.1%).

4. Conclusions

A method to obtain a single crystal large enough for neutron protein crystallography has been developed. In the present study, we have demonstrated this method, which is a combination of the use of a crystallization phase diagram and a crystal-quality assessment by X-ray diffraction. Moreover, it is suggested that the overall B factor is a convenient criteria for the X-ray assesment, since it is independent of the experimental conditions. This method should be applicable to not only the production of large crystals for neutron analysis but also of good-quality crystals for atomic resolution X-ray analysis. 2.4 Å neutron data could be collected using a 1.7 mm^3 crystal obtained under the optimum conditions. The neutron structural analysis is still in progress and full details of the structure determination will be reported shortly.

This work was supported in part by an 'Organized Research Combination System' Grant from the Ministry of Education, Culture, Sports, Science and Technology, Japan.

References

Brünger, A. T., Adams, P. D., Clore, G. M., DeLano, W. L., Gros, P., Grosse-Kunstleve, R. W., Jiang, J.-S., Kuszewski, J., Nilges, N., Pannu, N. S., Read, R. J., Rice, L. M., Simonson, T. & Warren, G. L. (1998). *Acta Cryst.* D**54**, 905–921.

Collaborative Computational Project, Number 4 (1994). *Acta Cryst.* D**50**, 760–763.

Habash, J., Raftery, J., Nuttall, R., Price, H. J., Wilkinson, C., Kalb, A. J. & Helliwell, J. R. (2000). *Acta Cryst.* D**56**, 541–550.

Helliwell, J. R. (1997). *Nature Struct. Biol.* **4**, 874–876.

Hittel, D. S. & Voordouw, G. (2000). *Antonie van Leeuwenhoek; J. Microbiol. Serol.* **77**, 13–22.

Mizuno, N., Hittel, D. S., Miki, K., Voordouw, G. & Higuchi, Y. (2000). *Acta Cryst.* D**56**, 754–755.

Mizuno, N., Hittel, D. S., Voordouw, G. & Higuchi, Y. (2002). *Acta Cryst.* A**58**, C304.

Mizuno, N., Voordouw, G., Miki, K., Sarai, A. & Higuchi, Y. (2003). In the press.

Niimura, N. (1999). *Curr. Opin. Struct. Biol.* **9**, 602–608.

Niimura, N., Chatake, T., Ostermann, A., Kurihara, K. & Tanaka, I. (2003). *Z. Kristallogr.* **218**, 96–107.

Otwinowski, Z. & Minor, W. (1997). *Methods Enzymol.* **276**, 307–326.

Riès-Kautt, M. & Ducruix, A. (1992). *Crystallization of Nucleic Acids and Proteins*, edited by A. Ducruix & R. Giegé, pp. 195–218. Oxford University Press.

Schoenborn, B. P. (1985). *Methods Enzymol.* **114**, 510–529.

Tanaka, I., Kurihara, K., Chatake, T. & Niimura, N. (2002). *J. Appl. Cryst.* **35**, 34–40.

Tsyba, I. & Bau, R. (2002). *Chemtracts*, **15**, 233–257.

Wilson, A. J. C. (1942). *Nature (London)* **150**, 151–152.